

Electronic Structure of the Two-Leg Spin Ladder $(C_5H_{12}N)_2CuBr_4$ Pere Alemany,^{*,†} Antonio Rodríguez-Forteza,[‡] and Enric Canadell^{*,§}[†]Departament de Química Física and Institut de Química Teòrica i Computacional (IQTCUB), Universitat de Barcelona, Diagonal 647, 08028 Barcelona, Spain[‡]Departament de Química Física i Inorgànica, Universitat Rovira i Virgili, Marcel·lí Domingo s/n, 43007 Tarragona, Spain[§]Institut de Ciència de Materials de Barcelona (ICMAB-CSIC), Campus UAB, 08193 Bellaterra, Spain

ABSTRACT: A density functional theory study of the two-leg spin ladder $(C_5H_{12}N)_2CuBr_4$ reveals antiferromagnetic interactions through the rungs and legs, although the latter are significantly smaller. Our work suggests interest in manipulating the physical behavior of this prototypical system by doping or chemical modifications.

Is(piperidinium) tetrabromocuprate(II), $(C_5H_{12}N)_2CuBr_4$, containing coupled spin $1/2$ Heisenberg antiferromagnetic (AF) ladders,¹ is one of the most interesting spin-ladder materials. Different physical measurements^{2–5} agree in qualifying this material as a prototypical two-leg spin ladder,⁶ which thus may be important in testing some issues related to the spin Luttinger liquid and Bose–Einstein condensation in magnetic insulators.⁷ Here we report a first-principles density functional theory (DFT) study concerning the strength of the magnetic interactions and how they are influenced by the nature of the halogen, counterion, and structural details.

In the crystal structure of this material,¹ distorted $CuBr_4^{2-}$ tetrahedra form chains of weakly interacting dimeric units (Figure 1). Two $Br \cdots Br$ (4.10 Å) contacts link each monomer into magnetic dimers. These form a double chain running along the *a* axis with $Br \cdots Br$ contacts of 4.31 Å between dimers. The sum of the van der Waals (vdW) radii of a pair of Br atoms is 3.70 Å, so that these $Br \cdots Br$ distances are very long. The $CuBr_4^{2-}$ tetrahedra in each dimer are related by a center of inversion, making the two Cu^{II} ions crystallographically and magnetically equivalent. Neighboring chains of dimers related by a *c*-glide operation form layers in the *ac* planes (Figure 1). The shortest $Br \cdots Br$ contacts (5.79 Å) between neighboring chains are long enough to neglect interchain interactions. The organic cations form a network of bridging hydrogen bonds between the $CuBr_4^{2-}$ tetrahedra. The complete crystal structure can be obtained by the stacking of layers of double chains perpendicular to the *b* direction, and the repeat unit of the solid contains two such layers. The shortest interlayer $Br \cdots Br$ contacts (5.66 Å) ensure that the chains are also well isolated in the direction perpendicular to the layers.

First-principles spin-polarized calculations were carried out using a numerical atomic orbital DFT approach⁸ implemented in the SIESTA code.⁹ The generalized gradient approximation (GGA) and, in particular, the Perdew–Burke–Ernzerhof (PBE) functional,¹⁰ as well as norm-conserving scalar relativistic pseudopotentials¹¹ factorized in the Kleinman–Bylander form,¹² were used. Because of the large size (385 atoms) of the double unit cell

needed to extract the coupling constants, it is important to establish computational settings providing reliable values at a reasonable computational cost. Detailed tests concerning convergence with respect to a basis set and grid of *k* points were carried out. A basis set with split-valence triple- and double- ζ basis sets including polarization orbitals for Cu and Br, respectively, and a split-valence double- ζ basis set for the atoms in the organic cation (C, H, N), as obtained with energy shifts of 50 meV for Cu and Br and 100 meV for C, H, and N,¹³ were selected together with a $4 \times 2 \times 4$ *k*-point mesh.¹⁴ To ensure an accuracy of 1 K for the calculated coupling constants, the convergence criterion for the elements of the density matrix was set to 10^{-6} . The energy cutoff of the real-space integration mesh was 200 Ry. The room temperature experimental crystal structure was used in all calculations. Calculations for discrete dimers were carried out by adopting the hybrid B3LYP functional¹⁵ using the *Gaussian 03* code.¹⁶ Basis sets of triple- ζ quality for Cu and double- ζ quality for all other atoms were used.¹⁷

Using a single cell, we obtain a value for the exchange coupling constant within the dimers, J_{rung} of -33.0 K, which is slightly larger than twice the experimental value obtained from fits of the magnetic susceptibility (-12.9 or -13.3 K).^{2–4,18} This is the same ratio that was found when comparing coupling constants calculated with GGA-type functionals and the hybrid B3LYP functional, which is well-known to reproduce accurately the experimental coupling constants.^{19,20} The coupling between tetrahedra in different layers is very small (-0.2 K) and in any case below the accuracy in our calculations (~ 1 K). To obtain a value for the exchange coupling constant for the legs of the spin ladder, we used a supercell with a doubled unit cell in the *a* direction for which we find $J_{\text{rung}} = -33.3$ K, practically the same value as that obtained from the single-cell calculations, and $J_{\text{leg}} = -3.3$ K, which compares pretty well with the experimental result (-3.6 or -3.8 K),^{2–4} an agreement that, in view of the small value, is most probably due to some error compensation. The calculated ratio of rung-to-leg coupling constants is thus 10; i.e., the coupling within the dimers is significantly larger than that between dimers, in good agreement with experiments.^{2–4}

Even-leg spin ladders are good candidates to induce superconductivity from an insulating state by injecting a small number of carriers^{6,21} provided that there is a nonnegligible energy dispersion. Thus, we calculated the band structure of $(C_5H_{12}N)_2CuBr_4$ to see if, despite the long $Br \cdots Br$ distances between tetrahedra, the system acquires some band dispersion. Shown in Figure 2 is the band structure for the most stable configuration of the single

Received: April 2, 2011

Published: June 17, 2011

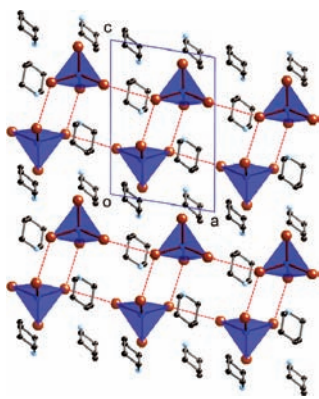


Figure 1. Crystal structure of $(\text{C}_5\text{H}_{12}\text{N})_2\text{CuBr}_4$ viewed along the b axis showing one layer of CuBr_4^{2-} tetrahedra. H atoms are not shown for clarity.

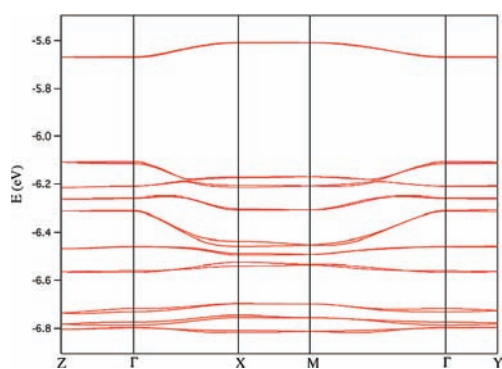


Figure 2. AF band structure calculated for $(\text{C}_5\text{H}_{12}\text{N})_2\text{CuBr}_4$ using a single unit cell. $\Gamma = (0, 0, 0)$, $X = (\frac{1}{2}, 0, 0)$, $Y = (0, \frac{1}{2}, 0)$, $Z = (0, 0, \frac{1}{2})$, and $M = (\frac{1}{2}, 0, \frac{1}{2})$ in units of the monoclinic reciprocal lattice.

unit cell. For simplicity, we have chosen this spin configuration, which leads to ferromagnetic instead of AF interactions along the legs (but an AF interaction within the rung), to avoid doubling of the number of bands and because the smallness in the strength of the interaction along the legs hardly introduces any significant change with respect to that of the fully AF state. All bands in Figure 2 are, of course, a couple of identical bands associated with the spin-up and spin-down electrons, each located on one of the two different but equivalent CuBr_4 tetrahedra of the spin ladder.

It is clear that there is some dispersion in the direction of the chains ($\Gamma \rightarrow X$), whereas the bands are almost completely flat along the b^* and c^* directions. The bands shown in Figure 2 are those formally based on the d orbitals of copper. Those at around -6.1 eV are the highest filled ones. The two bands around -5.7 eV are thus empty for a $\text{Cu}^{\text{II}} d^9$ configuration. It is quite remarkable that, despite the very large $\text{Cu} \cdots \text{Cu}$ distances and tetrahedral separation (i.e., $\text{Br} \cdots \text{Br}$ distances considerably larger than the sum of the vdW radii), some bands, including the highest filled and lowest empty ones, exhibit a nonnegligible dispersion. Note that the upper filled bands undergo two avoided crossings with lower bands, so that the intended dispersion is around 0.2 eV. When one looks at the orbital nature of these bands, it is found that, although they are formally based on Cu d levels, there is a large delocalization toward the Br atoms, which are those implicated in the contacts along the ladder direction.

Such delocalization is clearly evidenced by calculation of the spin densities, which are quite delocalized over the whole CuBr_4^{2-} tetrahedron, with as much as 60% of the unpaired electrons on the Br atoms. Such delocalization is essential for the calculated nonnegligible band dispersion. In view of this observation and the prototypical even-leg ladder behavior, it would be of utmost interest to undertake chemical doping studies of this phase by slightly altering the cationic network.

We also carried out calculations for the magnetic coupling constants of discrete dimeric units. The reason is 2-fold. First, it is by now quite well established^{19,20} that the best numerical accuracy for calculation of the exchange coupling constants is obtained when using the hybrid B3LYP functional.¹⁵ Because, for practical reasons, such calculations are not possible within the present periodic approach, we have carried them out for discrete units. Given the structural and physical details discussed above, this discrete approach should be appropriate here. Second, by doing discrete calculations, we do not need to keep the electro-neutrality of the system and we can test the possible role of cations.²⁰

The J_{rung} and J_{leg} coupling constants were calculated both without the cations ($[(\text{CuBr}_4)_2]^{4-}$ dimeric units) and including them (the same dimeric units and two cations as those found in the crystal, i.e., $[(\text{CuBr}_4)_2(\text{C}_6\text{H}_5\text{N})_2]^{2-}$ discrete units). The calculated values were found to be (in K) $J_{\text{rung}} = -16.5$ and $J_{\text{leg}} = -11.0$ without cations and $J_{\text{rung}} = -14.3$ and $J_{\text{leg}} = -0.3$ upon inclusion of the cations. Thus, whereas J_{rung} , which is always larger in absolute value, is practically unaffected by inclusion of the cations, this is not the case for J_{leg} . The calculated value for J_{rung} denotes AF interaction and is in very good agreement with the experimental values. Considering the coupling along the legs, it is observed that, without inclusion of the cations, the $J_{\text{rung}}/J_{\text{leg}}$ ratio is smaller than 2. In contrast, when they are included, J_{leg} is more than one order of magnitude smaller, pointing to a clear influence of the cation on the ratio of magnetic couplings. It is important to remark also that the tiny value of J_{leg} causes small absolute errors in its prediction (a few Kelvin) to lead to very different $J_{\text{rung}}/J_{\text{leg}}$ ratios. That $J_{\text{rung}}/J_{\text{leg}} > 1$ can be easily rationalized by comparing the spin densities for the two models. As for the periodic calculations, the spin density is largely delocalized toward the Br atoms. A larger spin density is found on the nearest Br atoms of the two tetrahedra that are in the rung. This is also true for the periodic calculations. These two tetrahedra are associated with two short $\text{Br} \cdots \text{Br}$ distances, whereas there is only one between two tetrahedra in the leg. Moreover, the shortest $\text{Br} \cdots \text{Br}$ distances are noticeably smaller in the rung than in the leg. In addition, inclusion of the positive cations subtly relocates part of the charge and spin density toward the outer Br atoms of the ladder at the expense of one of the Br atoms implicated in the interaction through the legs. This hardly affects the interaction in the rung but considerably decreases the interaction through the legs. In the absence of the cations, the coupling constants are more similar because all Cu–Br bond lengths are quite comparable and the spin density is more uniformly distributed between the four Br atoms. Thus, the nature and location of the cation subtly affects the magnetic coupling through the legs, which again suggests the possibility of exerting some chemical control on the physics of this system by cation manipulation.

Finally, we considered how the nature of the halogen could affect these results. $(\text{C}_5\text{H}_{12}\text{N})_2\text{CuCl}_4$ is also known and is isostructural with $(\text{C}_5\text{H}_{12}\text{N})_2\text{CuBr}_4$.²² The periodic GGA calculations for this

salt led to values of $J_{\text{rung}} = -10.9$ K and $J_{\text{leg}} = -1.9$ K, i.e., a severe decrease (between 2 and 3 times smaller) with respect to the values for $(\text{C}_5\text{H}_{12}\text{N})_2\text{CuBr}_4$, something that was corroborated by calculations for the discrete models. The more likely reasons for this reduction are (i) a smaller delocalization of the unpaired spin within the CuCl_4^{2-} units and (ii) a less favorable crystal packing. The GGA periodic calculations led to values of the spin density that are only marginally different from those found for the CuBr_4^{2-} units. The average spin density of the halogen atoms is 0.15 for the bromine compound and 0.13 for the chlorine compound. This very small decrease in the spin density cannot be the driving force for the severe reduction in the magnetic interactions. Thus, we suspect that the reason must be found in the details of the crystal packing. Indeed, analysis of the crystal structure shows that in the chlorine compound the $\text{Cl}\cdots\text{Cl}$ close contacts, which are 4.11 Å in the rung and 4.21 Å in the legs, are 0.61 and 0.71 Å longer than the sum of the vdW radii of a pair of Cl atoms (3.50 Å). In the bromine compound, the corresponding values are only 0.40 and 0.61 Å, respectively. This means that the vdW interactions in these salts are less favorable for chlorine than for bromine pairs. This leads to the comparatively longer $\text{X}\cdots\text{X}$ distances and, consequently, to noticeably smaller magnetic coupling constants for the chlorine compound. Thus, it would be very interesting to explore isostructural systems with $\text{CuCl}_x\text{Br}_{4-x}$ mixed-halogen tetrahedral anions. The difference in the $\text{X}\cdots\text{H}$ ($\text{X} = \text{Br}, \text{Cl}$) hydrogen-bond strength may be enough to avoid disorder and selectively change the $J_{\text{rung}}/J_{\text{leg}}$ ratio by modifying the $\text{X}\cdots\text{X}$ contacts. In view of the hydrogen-bonding network, the CuBr_2Cl_2 salt appears especially appealing.

In summary, the present first-principles computations suggest that $(\text{C}_5\text{H}_{12}\text{N})_2\text{CuBr}_4$ may be susceptible to chemical manipulations that could bring extremely interesting variations in the physical properties of this remarkable prototypical even-leg spin-ladder material.

AUTHOR INFORMATION

Corresponding Author

*E-mail: p.alemany@ub.edu (P.A.), canadell@icmab.es (E.C.).

ACKNOWLEDGMENT

We thank P. Batail for suggesting this work and his comments. This work was supported by DGI-Spain (Grants CSD2007-00041, FIS2009-12721-C04-03, CTQ2008-06670-C02-02/BQU, and CTQ2008-06549-C02-01/BQU), Generalitat de Catalunya (Grants 2009 SGR 1459 and 2009 SGR 462), and XRQTC. A. R.-F. acknowledges support through the Ramón y Cajal program (DGI-Spain).

REFERENCES

- (1) Patyal, B. R.; Scott, B. L.; Willett, R. D. *Phys. Rev. B* **1990**, *41*, 1657.
- (2) Watson, B. C.; Kotov, V. N.; Meisel, M. W.; Hall, D. W.; Granroth, G. E.; Montfrooij, W. T.; Nagler, S. E.; Jensen, D. A.; Backov, R.; Petruska, M. A.; Fanucci, G. E.; Talham, D. R. *Phys. Rev. Lett.* **2001**, *86*, 5168.
- (3) Lorenz, T.; Heyer, O.; Garst, M.; Anuso, F.; Rosch, A.; Rüegg, Ch.; Krämer, K. W. *Phys. Rev. Lett.* **2008**, *100*, 067208.
- (4) Klanjsek, M.; Mayaffre, H.; Berthier, C.; Horvatic, M.; Chiari, B.; Piovesana, O.; Bouillot, P.; Kollath, C.; Orignac, E.; Citro, R.; Giamarchi, T. *Phys. Rev. Lett.* **2008**, *101*, 137207.

- (5) Thielemann, B.; Rüegg, Ch.; Rønnow, H. M.; Läuchli, A. M.; Caux, J.-S.; Normand, B.; Biner, D.; Krämer, K. W.; Güdel, H.-U.; Stahn, J.; Habicht, K.; Kiefer, K.; Boehm, M.; McMorrow, D. F.; Mesot, J. *Phys. Rev. Lett.* **2009**, *102*, 107204.
- (6) Dagotto, E. *Rep. Prog. Phys.* **1999**, *62*, 1525.
- (7) Giamarchi, T.; Rüegg, Ch.; Tschernyshyov, O. *Nat. Phys.* **2008**, *4*, 198.
- (8) (a) Hohenberg, P.; Kohn, W. *Phys. Rev.* **1964**, *136*, 864. (b) Kohn, W.; Sham, L. J. *Phys. Rev.* **1965**, *140*, 1133.
- (9) Soler, J. M.; Artacho, E.; Gale, J. D.; García, A.; Junquera, J.; Ordejón, P.; Sánchez-Portal, D. *J. Phys.: Condens. Matter* **2002**, *14*, 2745.
- (10) Perdew, J. P.; Burke, K.; Ernzerhof, M. *Phys. Rev. Lett.* **1996**, *77*, 3865.
- (11) Trouiller, N.; Martins, J. L. *Phys. Rev. B* **1991**, *43*, 1993.
- (12) Kleinman, L.; Bylander, D. M. *Phys. Rev. Lett.* **1982**, *48*, 1425.
- (13) Artacho, E.; Sánchez-Portal, D.; Ordejón, P.; García, A.; Soler, J. M. *Phys. Status Solidi B* **1999**, *215*, 809.
- (14) Monkhorst, H. J.; Park, J. D. *Phys. Rev. B* **1976**, *13*, 5188.
- (15) Becke, A. D. *J. Chem. Phys.* **1993**, *98*, 5648.
- (16) Frisch, M. F.; et al. *Gaussian 03*, revisions B.4 and C.1; Gaussian Inc.: Pittsburgh, PA, 2003.
- (17) Schaefer, A.; Huber, C.; Ahlrichs, R. *J. Chem. Phys.* **1994**, *100*, 5829.
- (18) $\hat{H} = -\sum[J_{\text{rung}}\vec{S}_{i,1}\cdot\vec{S}_{i,2} + J_{\text{leg}}(\vec{S}_{i,1}\cdot\vec{S}_{i+1,1} + \vec{S}_{i,2}\cdot\vec{S}_{i+1,2})]$ is used.
- (19) (a) Ruiz, E.; Alemany, P.; Alvarez, S.; Cano, J. *J. Am. Chem. Soc.* **1997**, *119*, 1297. (b) Ruiz, E.; Cano, J.; Alvarez, S.; Alemany, P. *J. Comput. Chem.* **1999**, *20*, 1391.
- (20) Jornet-Somoza, J.; Deumal, M.; Landee, C. P.; Turnbull, M. M.; Novoa, J. J. *Inorg. Chem.* **2010**, *49*, 8017 and references cited therein.
- (21) Giamarchi, T. *Quantum Physics in One Dimension*; Oxford University Press: Oxford, U.K., 2004; Chapter 8.
- (22) Fernandez, V.; Moran, M.; Gutierrez-Rios, M. T.; Foces-Foces, C.; Cano, F. H. *Inorg. Chim. Acta* **1987**, *128*, 239.